

## Global Kinetic Constants for Thermal Oxidative Degradation of a Cellulosic Paper

TAKASHI KASHIWAGI and HIDESABURO NAMBU\*

*Building and Fire Research Laboratory, National Institute of Standards and Technology,  
Gaithersburg, MD 20899*

Values of global kinetic constants for pyrolysis, thermal oxidative degradation, and char oxidation of a cellulosic paper were determined by a derivative thermal gravimetric study. The study was conducted at heating rates of 0.5, 1, 1.5, 3, and 5°C/min in ambient atmospheres of nitrogen, 0.28%, 1.08%, 5.2% oxygen concentrations, and air. Sample weight loss rate, concentrations of CO, CO<sub>2</sub>, and H<sub>2</sub>O in the degradation products, and oxygen consumption were continuously measured during the experiment. Values of activation energy, pre-exponential factor, orders of reaction, and yields of CO, CO<sub>2</sub>, H<sub>2</sub>O, total hydrocarbons, and char for each degradation reaction were derived from the results. Heat of reaction for each reaction was determined by differential scanning calorimetry. A comparison of the calculated CO, CO<sub>2</sub>, H<sub>2</sub>O, total hydrocarbons, sample weight loss rate, and oxygen consumption was made with the measured results using the derived kinetic constants and accuracy of the values of kinetic constants was discussed.

### INTRODUCTION

This study is a part of a project in which ignition and subsequent flame spread over a thin sheet of paper in a microgravity environment is being studied and modeled. The model requires a large amount of information on physical and chemical processes of the paper as inputs. However, the model describes a time-dependent axisymmetric configuration with flow motion and mass and heat transport, which requires a large quantity of computational time. The degree of accuracy in the condensed phase should be consistent with that in the gas phase. In the gas phase, at present, one-step global gas phase oxidation reaction was used [2]. Therefore, a global approach to the thermal degradation reactions in the condensed phase was used in this study. However, our previous studies showed that the values of global thermal degradation kinetic constants of the paper affected smoldering [1], ignition, and the transition from ignition to flame spread [2]. Therefore, the measurement of these quantities with a reasonable accuracy is needed to predict ignition and flame spread behavior of the paper in microgravity. The calculated results will be compared with experimental data that will be obtained by potential

experiments in a spacecraft or using a drop tower. Finally, the model could be used for fire safety in a spacecraft where there is a potential fire hazard from various papers [3].

There are numerous studies on the thermal degradation of cellulose and wood. Reviews were given by Shafizadeh [4] and his co-workers [5]; this study is concentrated on how to express mass addition rates from a thermally degrading paper to the gas phase, which affects flow motion near the surface in microgravity [1, 2]. Although inert evolved degradation products such as CO<sub>2</sub> and H<sub>2</sub>O do not participate in gas-phase oxidative reactions, they dilute oxygen near the surface by pushing oxygen away from the surface in microgravity [1] and affect transition from ignition to flame spread [2]. Therefore, it is important to measure generation rates of both combustible gases and inert gases during the degradation period. There are numerous different hydrocarbon gases in the degradation products from cellulosic materials [6, 7] and kinetic constants of all these gas-phase oxidation reactions have not been measured. Furthermore, the gas-phase oxidation reaction in the current model is assumed to be a one-step reaction. (In future two oxidative reactions, one for total hydrocarbons and the other for CO will be considered.) Therefore, at present there is no need to analyze and quantify all the differing hydrocarbons in the degradation prod-

\* Guest researcher from Nihon University, Tokyo Japan.

ucts. The measurement of concentrations of CO, CO<sub>2</sub>, H<sub>2</sub>O, and total hydrocarbons in the evolved degradation products are needed. Since the ambient atmosphere in a spacecraft is air or 30% oxygen concentration (during an extravehicular activity) [3], not only pyrolysis reactions but also oxidative reactions should be included. Although there are published results for kinetic constants of oxidation reactions [8–12, 18] measured in air, in all but one [12] the effects of simultaneously occurring pyrolysis reactions are included in the derived values. Furthermore, these studies did not measure generation rates of evolved gaseous degradation products.

In this study the oxygen dependency of the kinetic constants is determined by conducting measurements at various oxygen concentrations, similar to the work of Rogers and Ohlemiller [12] and in contrast to previous studies conducted only in air [8–11]. The competition between the overall pyrolysis reaction and oxidative degradation is examined by calculating each reaction rate at selected heating rates using the derived kinetic constants for the two reactions to determine whether the oxidative reaction is important under fire level heating rates.

## EXPERIMENTAL PROCEDURE

### Material

Initially an ashless filter paper was used as a test sample. However, radiative autoignition did not occur with this sample in preliminary experiments in normal gravity. This was due to the high reflectivity of the sample with respect to visible–near infrared emission spectra of the tungsten lamp used as the external thermal radiation source in the experiment. Therefore, a black paper (office supply) was used in this study to increase the absorptivity of the external radiation,<sup>1</sup> although the sample is less pure than the filter paper. The sample was ground and 4–5 mg of powdered sample was used in this study.

<sup>1</sup> However, the subsequent measurement of surface reflectance indicates that reflectance increases significantly above 0.9  $\mu\text{m}$ , which indicates that a dye was used for its blackness instead of carbon black.

### Experimental Setup

A schematic illustration of the experimental setup is shown in Fig. 1. The thermal degradation characteristics were determined by thermogravimetry using a Mettler TA 12 thermoanalyzer.<sup>2</sup> Low heating rates (up to 5°C/min) were used in this study to ensure that heat transfer as well as mass transport processes of oxygen and degradation products through the sample did not affect the experimental results [13]. The samples were fine powders and were spread thinly over the bottom of a prebaked aluminum pan about 12 mm in diameter. The sample pan was set at the center of the sample support over the thermocouple, whose output was used to control the temperature of the furnace. The weight of the sample, its temperature, concentrations of CO, CO<sub>2</sub>, H<sub>2</sub>O, and O<sub>2</sub> in the exhaust gas,<sup>3</sup> and the time were simultaneously recorded by a computer. The consumption of O<sub>2</sub> by degradation of the sample was measured by the difference between the input O<sub>2</sub> concentration to the thermoanalyzer and the output O<sub>2</sub> concentration in the exhaust. This was accomplished by feeding the input gas to the reference cell of the oxygen analyzer and the output gas into the test gas cell of the analyzer. Then, the oxygen analyzer can be used to make a differential oxygen measurement and this analyzer has a capability to measure differential oxygen concentration in the range of 0%–0.5%. At first, a baseline run without a sample was conducted and then an identical run with a sample was repeated. The actual weight of the sample and concentrations of the gases were calculated from the difference between the sample run and the baseline run. This procedure removed the artificial change in the weight caused by buoyancy and slight drift in H<sub>2</sub>O analyzer by desorp-

<sup>2</sup> In order to adequately describe materials and equipment it is occasionally necessary to identify commercial products by manufacture's name. In no instance does such identification imply endorsement by the National Institute of Standards and Technology, nor does it imply that the particular product is necessarily the best available for that purpose.

<sup>3</sup> CO was measured by Siemens ULTRAMAT 4 (range 0–500 ppm), CO<sub>2</sub> by Siemens ULTRAMAT 5E (range 0–1000 ppm.), H<sub>2</sub>O by Siemens ULTRAMAT 5F (0–1000 ppm.), and O<sub>2</sub> by Siemens OXYMAT 5E (range in difference in oxygen concentration 0%–0.5%). All these instruments have reproducibility of  $\pm 0.1\%$ –1% of the span depending on the analyzer.

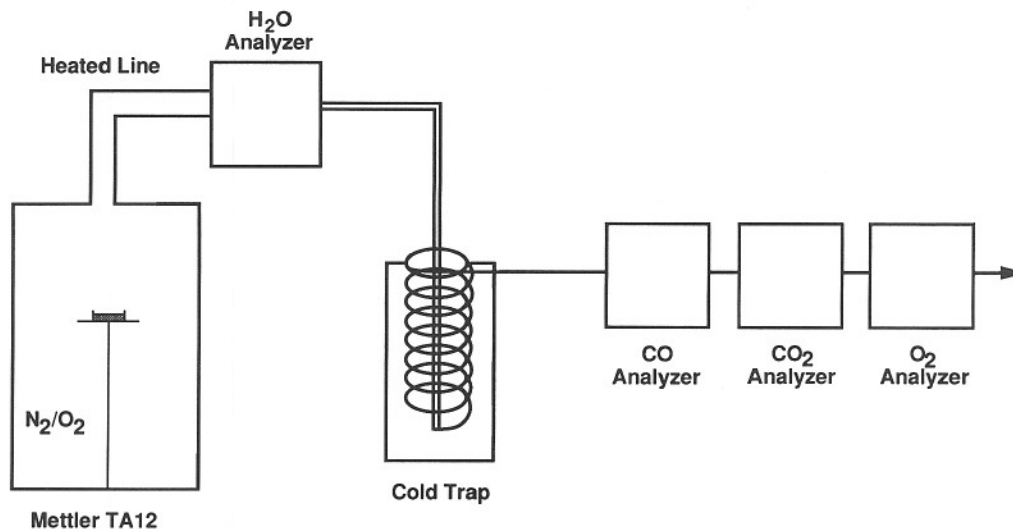


Fig. 1. Schematic illustration of experimental setup.

tion of absorbed H<sub>2</sub>O from the wall of the furnace generated by heating the furnace. The reproducibility of temperature for the peak sample weight loss rate was within 1°C.

The system was calibrated by conducting the degradation of a known amount of calcium oxalate, which degrades at about 130°C to generate only H<sub>2</sub>O, at about 490°C to generate only CO and CO<sub>2</sub>, and finally at about 670°C to generate only CO and CO<sub>2</sub>. Therefore, mass conservation of H<sub>2</sub>O through the system was examined from the sample weight loss and the measured H<sub>2</sub>O concentration in the exhaust gas. It was found that about 25% of water was lost between the degrading sample and the water analyzer, although the line between them was heated about 65°C. This loss was corrected in the data analysis. The system delay in response to H<sub>2</sub>O concentration change due to flow time and response time of the analyzer was measured at each heating rate and the data were shifted by a corresponding amount of delay at each heating rate during the data analysis. Similarly, the CO and CO<sub>2</sub> analysis systems were calibrated. Only the system delay was corrected for these two gases because mass conservation of these two gases was satisfied within 5%.

## RESULTS

### Pyrolysis Degradation Reaction

**Sample Weight Loss Rate.** The thermogravimetric study was conducted at heating rates of

0.5, 1, 1.5, 3, and 5°C/min in nitrogen and normalized weight loss rates are shown in Fig. 2 (Only the results at three heating rates are shown to avoid crowding the figure.) The derivative thermogravimetry (DTG) results were numerically obtained by taking the time derivative,  $d(W/W_0)/dt$ , of the ratio of the sample weight,  $W$ , to the initial sample weight,  $W_0$ , and their results were numerically smoothed. The trend in which temperature at peak weight loss rate increases with higher heating rate is consistent with theory in thermogravimetry [14]. The small increase in weight loss rate at a heating rate of 5°C/min near 430°C was noise in the data and should be ignored. Since there is one distinct peak in the DTG curve, the pyrolysis reaction is approximated to be a one-step global reaction instead of multiple steps, as published in previous studies [8, 15]. For the objective of this study this approximation is quite reasonable.

In order to determine kinetic constants for the global pyrolysis reaction, Kissinger's approach [16] was used for its simplicity, and it was best suited for the case with independent peaks without any overlapping of global reactions shown in Fig. 2. In this approach activation energy,  $E_p$ , and pre-exponential factor,  $A_p$ , can be determined without specifying order of reaction,  $n_p$  (When  $n_p$  is one, Kissinger's approach is exact. However, even if  $n_p$  is not one, it is still a good approximation [16]). The Kissinger plot for the global pyrolysis reaction is shown in Fig. 3. Here,  $dT/dt$  is heating rate and  $T_m$  is temperature in K at the peak sample weight loss rate. The

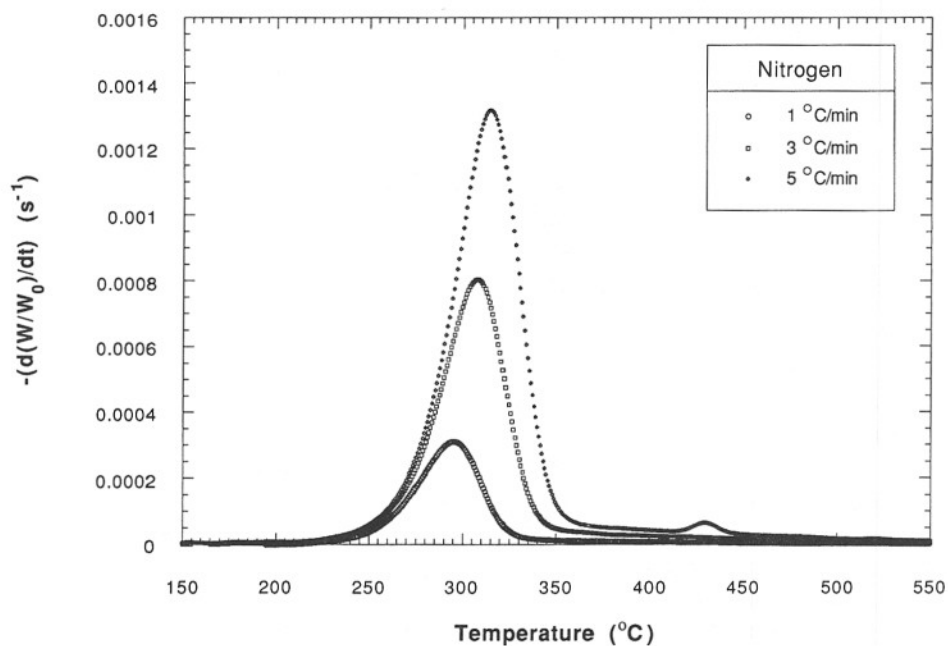


Fig. 2. Change in normalized sample weight loss rate with temperature at three different heating rates in nitrogen.

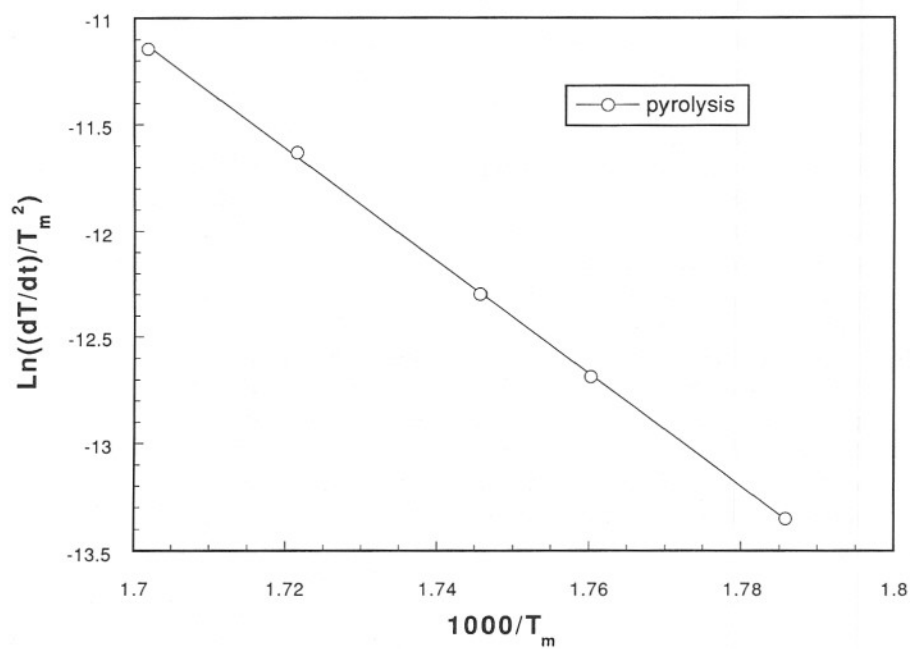


Fig. 3. Kissinger's plot in nitrogen to obtain pyrolysis kinetic constants.

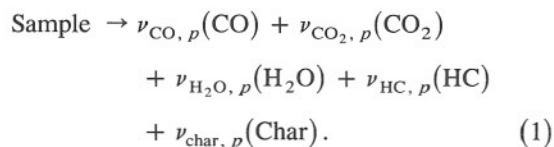
five data points shown in Fig. 3 correspond to the five heating rates used in this study. The slope of the fit is the value of activation energy divided by the gas constant,  $R$ , and the intercept value is  $\ln(A_p R/E_p)$ . The values obtained for  $E_p$  and  $A_p$  are summarized in Table 1. Then, order of reaction is determined using the determined values of  $E_p$  and  $A_p$  to best fit to the experimental weight loss rates shown in Fig. 2. The value obtained for  $n_p$  is 1.8, as indicated in Table 1. The calculated weight loss rates at heating rate of  $5^\circ\text{C}/\text{m}$  based on these values are close to the weight loss rates calculated by using kinetic values determined by Lewellen et al. [17]. The latter study used a heated screen at heating rates from 400 to  $1000^\circ\text{C}/\text{s}$ , and the order of reaction was assumed to be 1 instead of 1.8 in the present study. The value of peak weight loss rate calculated using the above kinetic constants determined from this study is within 10% of that calculated using kinetic constants determined by Ref. 17, but its peak weight loss occurs at about  $12^\circ\text{C}$  lower than the previous study. This small difference could be due to differences in the samples used in the two studies.

**Degradation Products.** The measured concentrations of  $\text{CO}$ ,  $\text{CO}_2$ , and  $\text{H}_2\text{O}$  gases in the evolved products at the three heating rates are shown in Figs. 4a, 4b, and 4c, respectively.  $\text{H}_2\text{O}$  concentration is the highest, followed by  $\text{CO}_2$ , and then  $\text{CO}$ . The  $\text{CO}$  and  $\text{CO}_2$  concentrations

show that slow char degradation continues over a wide temperature range after the pyrolysis reaction. However, the contribution from the char degradation is much smaller than from the pyrolysis reaction and it is approximated in this study that the char degradation contribution is negligible. This approximation helps to make the overall degradation model simple enough for the numerical calculation for ignition and flame spread to become within manageable computational time. For this reason, it is also approximated that the yields of these gases with respect to the sample weight loss are constant during the global pyrolysis reaction. Since the pyrolysis reaction consists of many individual reactions as pointed out above [4, 8], this approximation might severely reduce accuracy in predicting components in the degradation products. The consequence of this approximation on accuracy in concentrations of gaseous degradation products is described in the Discussion. Using the results shown in Figs. 4a–4c and Fig. 2, yields of each gas in the degradation products were calculated and best fitted yields values were selected. They are listed in Table 2.

Char yield is also approximated to be constant during the pyrolysis reaction, and its value was taken from the sample weight left after the sample was heated up to  $400^\circ\text{C}$ , assuming that the leftover sample was completely char. Char yield was not significantly affected by heating rate, which was observed by Suuberg and Dalal [18] and also in this study. However, it might be questionable to assume that char yield is constant during the entire pyrolysis reaction [8].

The yield of total hydrocarbons was determined from the mass balance among yields of  $\text{CO}$ ,  $\text{CO}_2$ ,  $\text{H}_2\text{O}$ , and char. Again, this yield was assumed to be constant during the pyrolysis period. The expression for the pyrolysis reaction is



The pyrolysis reaction rate,  $k_p$ , is expressed as

$$k_p = A_p (W_s/W_0)^{n_p} \exp(-E_p/RT), \quad (2)$$

where  $\nu_i$  is stoichiometric coefficient for species

**TABLE 1**  
Global Kinetic Constants

|                                |  |
|--------------------------------|--|
| Pyrolysis reaction             |  |
| $E_p$                          | 220 kJ/mol                             |
| $A_p$                          | $1.2 \times 10^{19} (\text{min}^{-1})$ |
| $n_p$                          | 1.8                                    |
| $\Delta H_p$                   | 570 J/g                                |
| Oxidative degradation reaction |  |
| $E_{\text{ox}}$                | 160 kJ/mol                             |
| $A_{\text{ox}}$                | $1.5 \times 10^{14} (\text{min}^{-1})$ |
| $n_{\text{ox}}$                | 0.5                                    |
| $n_{f,\text{ox}}$              | 1.3                                    |
| $\Delta H_{\text{ox}}$         | -5,700 J/g                             |
| Char oxidation reaction        |  |
| $E_{\text{char}}$              | 160 kJ/mol                             |
| $A_{\text{char}}$              | $3.4 \times 10^{11} (\text{min}^{-1})$ |
| $n_{\text{O}_2,\text{char}}$   | 0.78                                   |
| $n_{\text{char}}$              | 1                                      |
| $\Delta H_{\text{char}}$       | -25,000 J/g                            |

$i$ ,  $A_p$  is the pre-exponential factor,  $W_s$  is the sample weight (not including char weight),  $W_0$  is the initial sample weight,  $E_p$  is the activation energy, and  $R$  is the gas constant.

### Oxidative Degradation Reaction

**Sample Weight Loss Rate.** A thermogravimetric study was conducted in 0.28%, 1.08%,

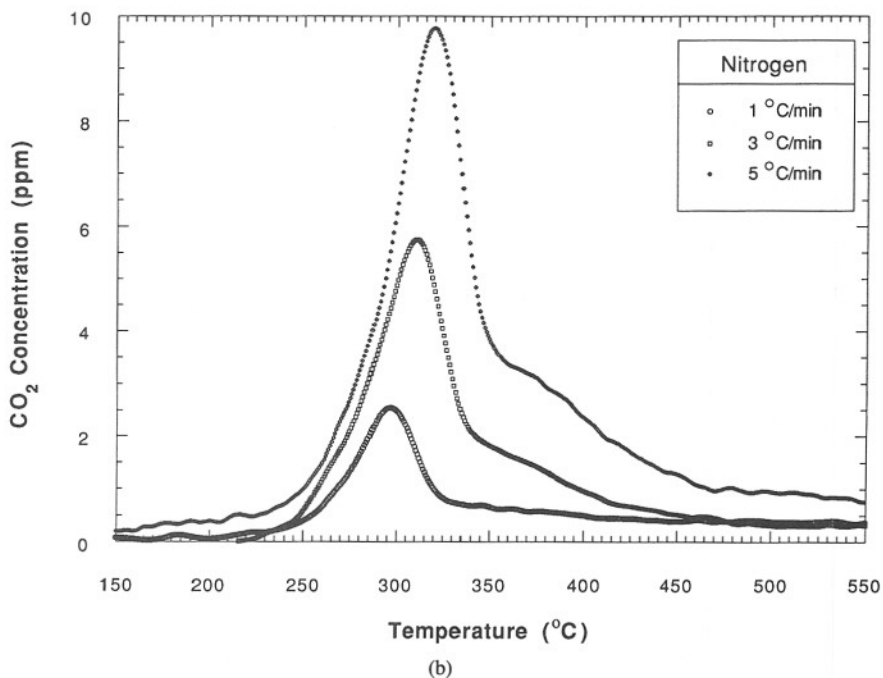
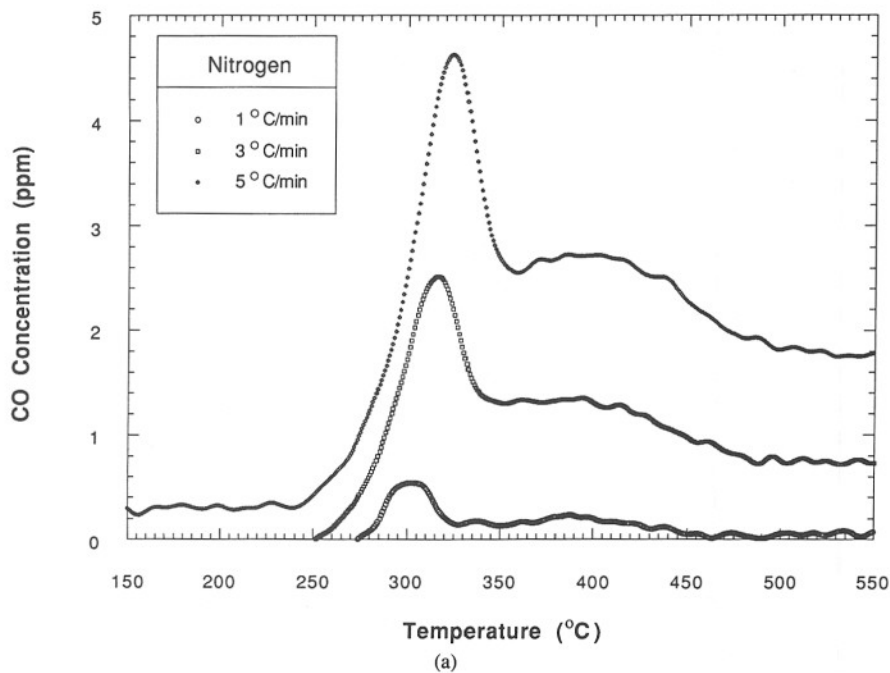
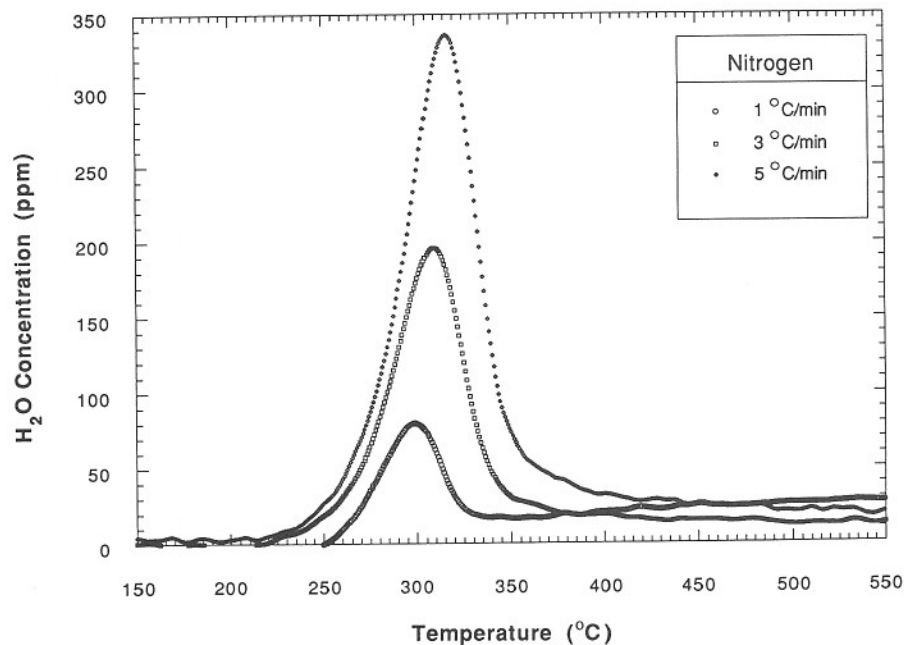


Fig. 4. CO, CO<sub>2</sub>, and H<sub>2</sub>O concentrations in evolved degradation products at three different heating rates in nitrogen, (a) CO, (b) CO<sub>2</sub>, and (c) H<sub>2</sub>O.



(c)

Fig. 4. (Continued).

5.2% of  $O_2/N_2$  mixtures and in air at heating rates of 1, 1.5, 3, and  $5^\circ\text{C}/\text{min}$ . Typical results of sample weight loss rate in air at the three heating rates are shown in Fig. 5. Comparison between the results in air and those in nitrogen (see Fig. 2) indicates that the first peak appeared at lower temperature in air than in nitrogen and there was a second peak at higher temperature in air. The first peak consisted of oxidative degradation and pyrolysis of the paper and the second peak was due to the char oxidation reaction. Therefore, kinetic constants for oxidative degradation of the paper could not be directly derived from the results shown in Fig. 5. If it was assumed that the oxidative degradation occurred independently with the pyrolysis degradation<sup>4</sup>, then kinetic constants for the oxidative degradation could be determined by subtracting pyrolysis components from the results. The pyrolysis component could be calculated from the above derived kinetic constants using measured temperature and sample weight at each

experimental point. Then, weight loss rate solely generated by the oxidative degradation was determined and the Kissinger plot for this using temperatures at the maximum weight loss rates were made for each oxygen concentration. The plots are shown in Fig. 6. As described above, the slope of each line is the value of activation energy. These values are tabulated in Table 3. It shows that the values for air and 5.2% oxygen concentration are close to each other, but the value increases with a decrease in oxygen concentration. The activation energy for 0.28% oxygen concentration is almost the same as that for pyrolysis degradation. Therefore, it is quite possible that the contribution at this oxygen level from the oxidative degradation could not be completely separated from the results of the pyrolytic degradation due to the small contribution of oxidative degradation. The results for 5.2% and air were mainly used for the determination of activation energy and 160 kJ/mol was selected for oxidative degradation.

The value for the pre-exponential factor for the oxidative degradation at oxygen concentrations of 1.08%, 5.2% and air was recalculated using the experimental data at  $5^\circ\text{C}/\text{m}$  and the above value of 160 kJ/mol for its activation energy. The

<sup>4</sup> Although many assumptions could be possible, this is the simplest one and also it allows that the obtained kinetic constants can apply *continuously* from an inert atmosphere to air.

TABLE 2

| Stoichiometric Coefficients (Mass Fraction) |      |
|---|------|
| Pyrolysis reaction                          |      |
| $\nu_{\text{H}_2\text{O}, p}$               | 0.5  |
| $\nu_{\text{CO}, p}$                        | 0.01 |
| $\nu_{\text{CO}_2, p}$                      | 0.03 |
| $\nu_{\text{HC}, p}$                        | 0.22 |
| $\nu_{\text{char}, p}$                      | 0.24 |
| Oxidative degradation reaction              |      |
| $\nu_{\text{O}_2, \text{ox}}$               | 0.41 |
| $\nu_{\text{H}_2\text{O}, \text{ox}}$       | 0.8  |
| $\nu_{\text{CO}, \text{ox}}$                | 0.08 |
| $\nu_{\text{CO}_2, \text{ox}}$              | 0.24 |
| $\nu_{\text{HC}, \text{ox}}$                | 0.08 |
| $\nu_{\text{char}, \text{ox}}$              | 0.21 |
| Char oxidation reaction                     |      |
| $\nu_{\text{O}_2, \text{char}}$             | 1.65 |
| $\nu_{\text{H}_2\text{O}, \text{char}}$     | 0.3  |
| $\nu_{\text{CO}, \text{char}}$              | 0.5  |
| $\nu_{\text{CO}_2, \text{char}}$            | 1.8  |
| $\nu_{\text{HC}, \text{char}}$              | 0.02 |
| $\nu_{\text{ash}, \text{char}}$             | 0.03 |

newly determined pre-exponential factor is plotted with respect to oxygen concentration in Fig. 7. The value at 0.28% oxygen concentration was not included due to large difference in activation energy between the experimentally determined

value (224 kJ/mol) and the selected value (160 kJ/mol). The curve fit indicates that the pre-exponential factor for the oxidative degradation is proportional to the 0.26 power of oxygen concentration. (However, the 0.5 power was used in this study for better fit to the experimental results, as is described later.) Order of reaction was determined from the best-fit data of the calculated sample weight loss rate for the oxidative degradation at four different heating rates in air. The value of 1.3 was obtained. This value does not necessarily mean actual order of chemical reaction and instead it only indicates the best-fit dependency on oxygen concentration. It is very difficult to compare these kinetic values with previous results due to differences in order of reaction. The calculated weight loss rates based on the kinetic constants shown in Table 1 are within a factor of five for the calculated results based on Rogers and Ohlemiller [12] and Shivadev and Emmons [19] at a temperature of 600 K without considering order of reaction.

**Degradation Products.** The results in air at three of the five heating rates are shown in Figs. 8a, 8b, and 8c, for CO, CO<sub>2</sub>, and H<sub>2</sub>O as

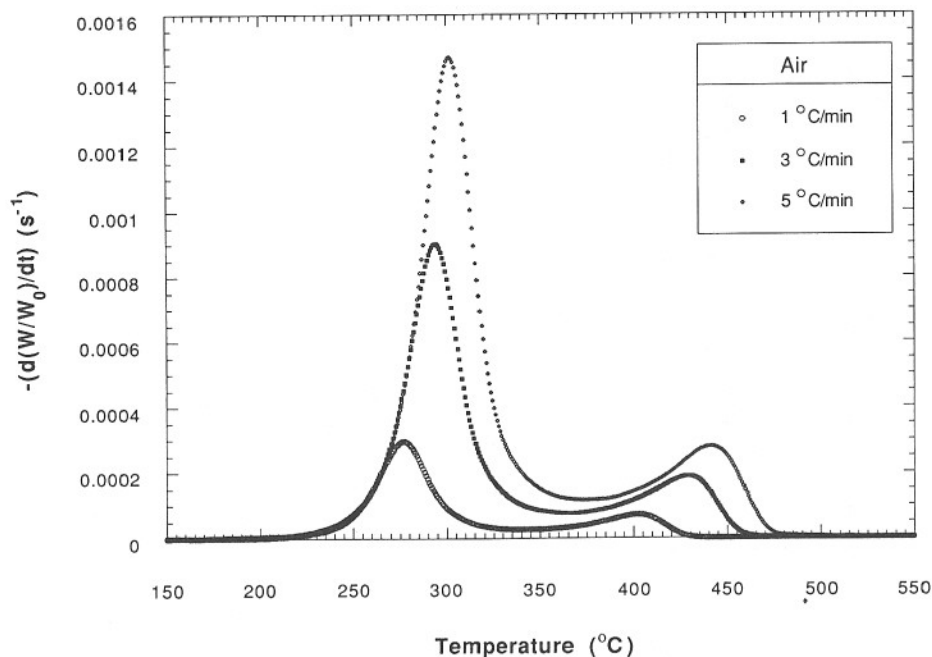


Fig. 5. Change in normalized sample weight loss rate with temperature at three different heating rates in air.

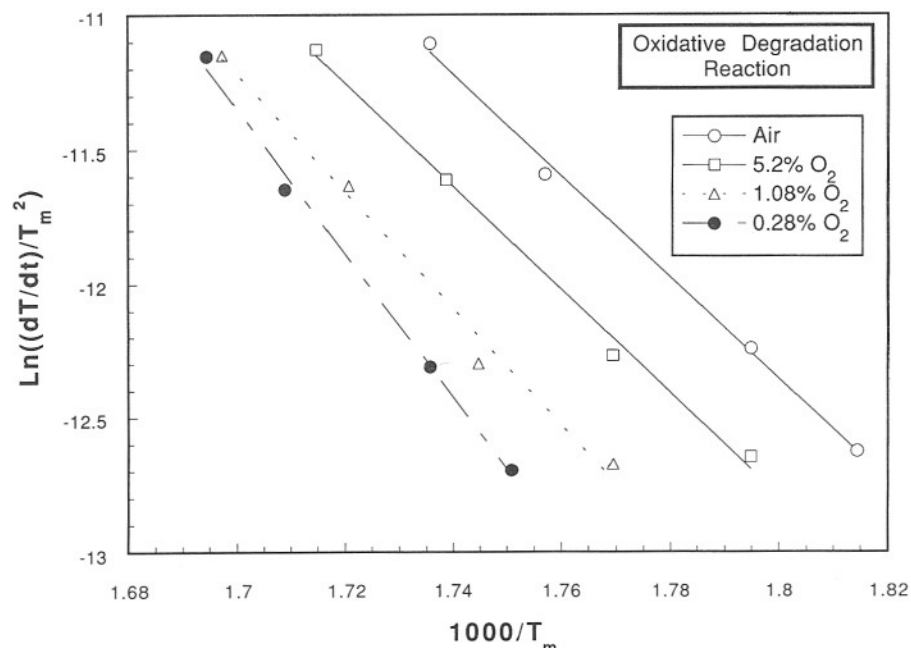


Fig. 6. Kissinger's plot in various ambient oxygen concentrations to obtain kinetic constants for oxidative degradation.

concentrations in the evolved degradation gases. The amount of CO increased about one order compared with the results in nitrogen shown in Fig. 4a. The CO generation by char oxidation was comparable to that by oxidative degradation. Similarly, CO<sub>2</sub> generation increased nearly one order compared with the results in nitrogen shown in Fig. 4b. More CO<sub>2</sub> was generated by char oxidation than by the oxidative degradation. The increase in evolved H<sub>2</sub>O in air was about a factor of 2 compared with the results in nitrogen shown in Fig. 4c. The generation of H<sub>2</sub>O by the char oxidation reaction was negligible. Since these products are generated from two global reactions of pyrolysis and oxidative degradation, those generated by oxidative degradation alone were calculated by subtracting the calculated generation of pyrolysis products based on measured sample

weight at any instant using the above-described pyrolysis kinetic constants and the yield of each product from the experimental data. Then yield of each product was best-fitted to the calculated concentration of each product; their values are listed in Table 2.

The yield of char was determined from the difference between calculated yield of char for pyrolysis degradation and measured char yield at the end of pyrolysis/oxidative degradations in the four different ambient oxygen concentrations (assuming that all samples left at the end of the pyrolysis/oxidative degradations were char). Its value is 0.21 as indicated in Table 2, which is close to 0.2 in the Shivadev and Emmons study [19]. The calculated amounts of total hydrocarbons obtained by subtracting masses of CO, CO<sub>2</sub>, and H<sub>2</sub>O from a sample weight loss and an addition of mass of oxygen consumed were unfortunately small negative values at higher temperatures instead of positive values. This was caused by subtracting and adding of masses with some inaccuracy in measurement. (Note that the experimental accuracy of the mass balance of CO, CO<sub>2</sub>, and H<sub>2</sub>O is about 5% and of oxygen consumption is within 10%.) The stoichiometric coefficient for oxygen was determined from the

TABLE 3

| Effects of Ambient Oxygen Concentration of $E_{ox}$ |                   |
|---|-------------------|
| Ambient Oxygen Concentration                        | $E_{ox}$ (kJ/mol) |
| Air   | 157               |
| 5.2%  | 160               |
| 1.08%   | 182               |
| 0.28%   | 224               |

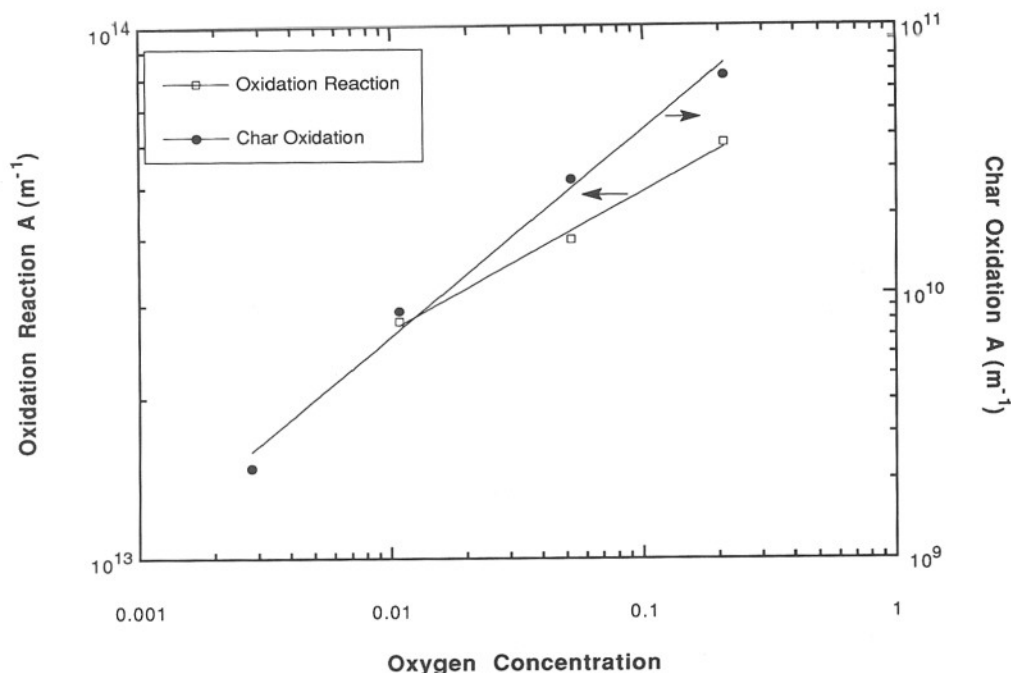
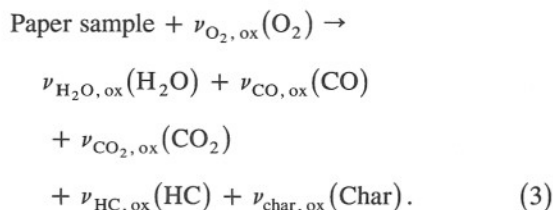


Fig. 7. Ambient oxygen concentration dependency of preexponential parameters.

measured consumption rates of oxygen and the calculated sample weight loss rate due to oxidative degradation. Then, the yield of total hydrocarbons was calculated by the overall mass balance among the degradation products and reactants (sample and oxygen). These values are summarized in Table 2. The expression for the oxidative degradation reaction is



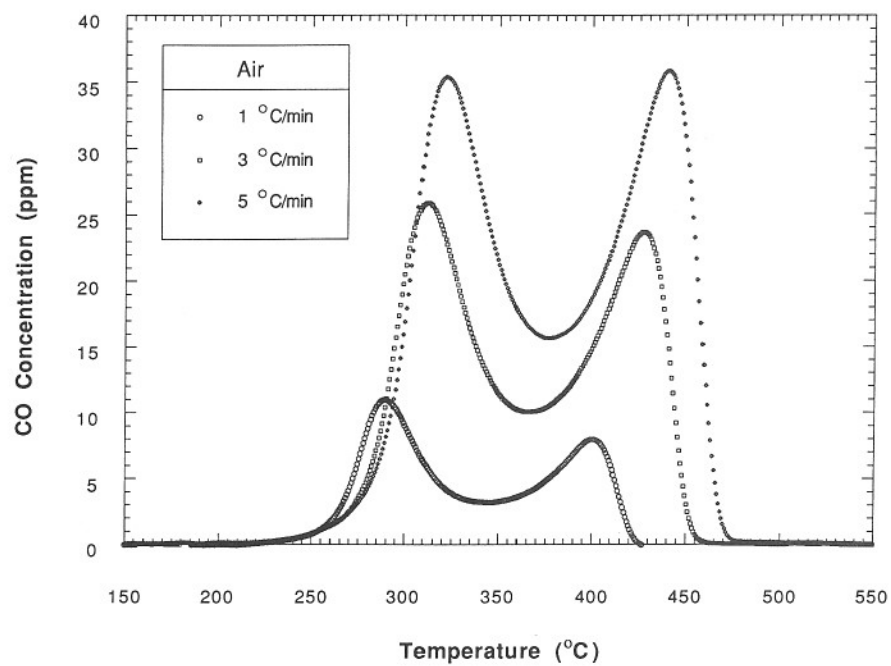
Oxidative degradation reaction rate,  $k_{\text{ox}}$ , is

$$\begin{aligned}
 k_{\text{ox}} = &A_{\text{ox}}(Y_{\text{ox}})^{n_{\text{ox}}}(W_s/W_0)^{n_{f, \text{ox}}} \\
 &\times \exp(-E_{\text{ox}}/RT), \quad (4)
 \end{aligned}$$

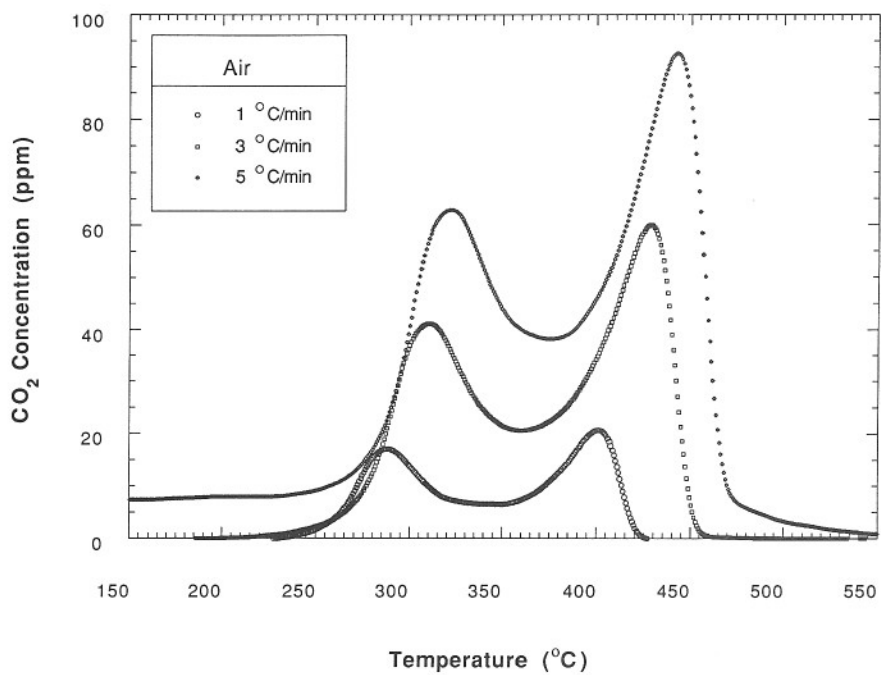
where  $Y_{\text{ox}}$  is the volume fraction of oxygen concentration and  $W_s$  is the sample weight (not including char weight).

### Char Oxidation Reaction

**Weight Loss Rate.** The results shown in Fig. 5 indicate that char oxidation could be expressed by a global one-step reaction. Using the above-described Kissinger approach, activation energy for the four different oxygen concentrations was determined by the Kissinger plot shown in Fig. 9. Here,  $T_m$  is temperature at which char weight loss rate of char oxidation is the maximum. (Note that all sample left after pyrolysis/oxidative degradations is assumed to be char.) The term  $dT/dt$  is heating rate of the char. The values obtained for the activation energy are listed in Table 4. Their values in 1.08% and 0.28% oxygen concentrations are lower than those in 5.2% oxygen concentration and air, similar to the case for oxidative degradation. With reduction in oxygen concentration, char oxidation rate decreases and becomes difficult to separate from slow pyrolysis of char. Another possibility is that the assumption of independent reaction between char pyrolysis and char oxidation might become more questionable in low oxygen concentration. Therefore, the value of 160 kJ/mol was selected for char oxidation, which was the value seen in

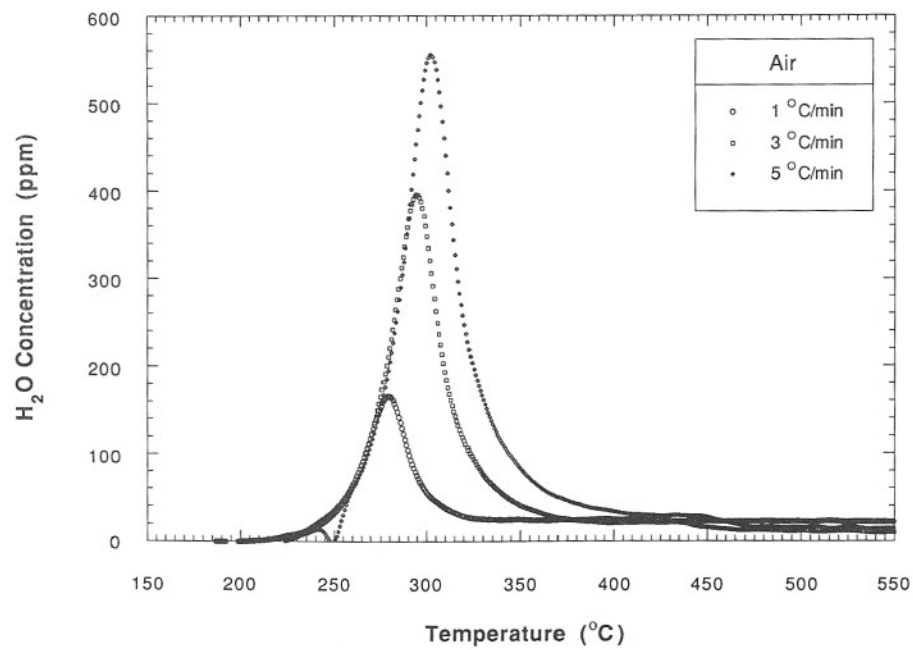


(a)



(b)

Fig. 8. CO, CO<sub>2</sub>, and H<sub>2</sub>O concentrations in evolved degradation products at three different heating rates in air, (a) CO, (b) CO<sub>2</sub>, and (c) H<sub>2</sub>O.



(c)

Fig. 8. (Continued).

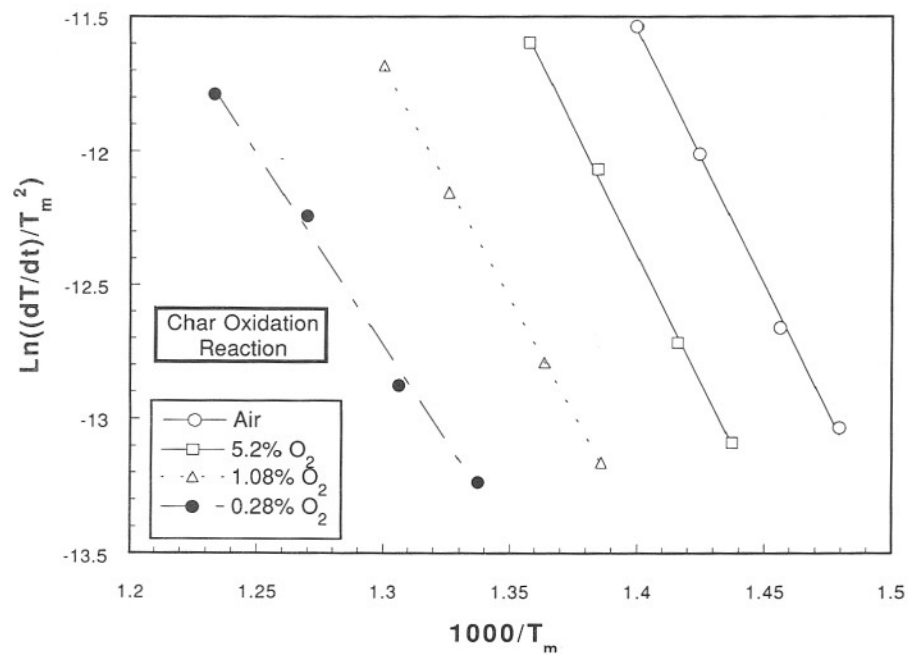


Fig. 9. Kissinger's plot in various ambient oxygen concentrations to obtain kinetic constants for char oxidation.

TABLE 4

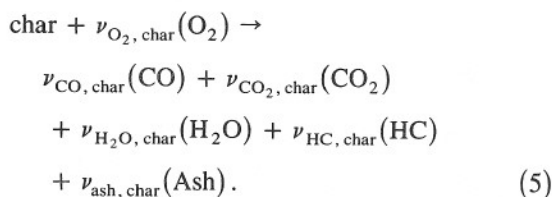
| Effects of Ambient Oxygen Concentration on $E_{\text{char}}$ |                            |
|--|----------------------------|
| Ambient Oxygen Concentration                                 | $E_{\text{char}}$ (kJ/mol) |
| Air  | 159                        |
| 5.2%   | 159                        |
| 1.08%  | 143                        |
| 0.28%  | 119                        |

5.2% oxygen concentration and air. The values for pre-exponential factor in 0.28% and 1.08% oxygen concentrations were adjusted by using 160 kJ/mol for activation energy to fit the experimental data at 5°C/m. Then, their oxygen concentration dependency was determined by plotting the values of pre-exponential factor with oxygen concentration, as shown in Fig. 7. The power of 0.78 was obtained from the slope of the best-fit curve. The determined kinetic constants are summarized in Table 1. Rogers and Ohlemiller [12] reported an activation energy of 163 kJ/mol and a pre-exponential value of  $4 \times 10^{10} \text{ min}^{-1}$  for their homogenized waste paper. Although the obtained activation energy in this study (160 kJ/mol) is very close to their value, the pre-exponential value in this study is about 9 times as large as their value. However, their order of reaction is quite different from first-order reaction determined by this study and it is difficult to directly compare the results obtained in this study with their results.

**Degradation Products.** The yields for CO, CO<sub>2</sub>, and H<sub>2</sub>O were determined from the measured concentrations of these gases in the evolved degradation products with the above determined global kinetic constants by selecting best-fit to the results shown in Figs. 8a–8c. Here, it was assumed that the yields of these gases were constant during char oxidation reaction. The yield of ash was determined from the leftover sample weight at the end of tests assuming that all leftover samples were ash. After determining the stoichiometric coefficient of oxygen from the amount of consumed oxygen during char oxidation, the yield of hydrocarbons was determined from the mass balance between the products and the reactants. However, the difference between the mass of reactants and the mass of products minus total hydrocarbons was so small that the accuracy of

the yield of total hydrocarbons is not high. The values of yields are summarized in Table 2.

The global char oxidation reaction is expressed as



The rate constant for char oxidation,  $k_{\text{char}}$ , is

$$\begin{aligned} k_{\text{char}} = A_{\text{char}} (Y_{\text{ox}})^{n_{\text{O}_2, \text{char}}} (W_{\text{char}} / W_0)^{n_{\text{char}}} \\ \times \exp(-E_{\text{char}} / RT), \end{aligned} \quad (6)$$

where  $W_{\text{char}}$  is weight of char.

### Heat of Reaction for the Three Global Degradation Reactions

Heat of reaction for each global degradation reaction was measured by differential scanning calorimetry (DSC). The measurement of heat of reaction pyrolysis degradation was conducted in nitrogen at the heating rate of 5°C/m. The measured heat release was divided by the sample weight lost during pyrolysis reaction. A small endothermic heat of 570 J/g was derived. The value of 370 J/g for pure cellulose was previously reported by Tang and Neil [20]. Considering the substantial composition difference in the sample, the difference in the two values might not be significant. For oxidative degradations the measurement was made in air at 5°C/m. Since in air endothermic pyrolysis and exothermic oxidative degradation occur simultaneously, the endothermic heat by pyrolysis reaction based on the calculated sample weight loss using the above described kinetic constants had to be corrected (added in this case) to the measured overall heat release. The corrected heat release was divided by the sample weight loss caused by oxidative degradation, which was derived from subtracting the calculated sample weight loss by pyrolysis reaction from the measured sample weight loss. An exothermic heat release of 5700 J/g was obtained. Heat of reaction for char oxidation was determined by the measured heat release divided by char weight loss and a large exothermic heat release of 25,000 J/g was obtained. These values

are comparable to the exothermic heat release of 4,200 J/g for oxidative degradation and 25,000 J/g for char oxidation reported by Rogers and Ohlemiller [12] for their homogenized waste paper study.

## DISCUSSION

Sample weight loss rates were calculated using the above determined kinetic constants for the three degradation reactions and compared with the measured data. Slight adjustments were made to values for  $A_{ox}$ ,  $n_{ox}$ , and  $A_{char}$  to fit better with the experimental data. Since values for  $A_{ox}$  and  $A_{char}$  were determined from the data fitted only at 5°C/m by keeping the same activation energy as described in the section on sample weight loss rates, the previously derived values for these parameters appear to need the adjustment. Final values are listed in Table 1.

The comparison of calculated sample weight loss rate with the experimental data in nitrogen at 3°C/m is shown in Fig. 10a as a typical example. The agreement is good enough for the objective of this study. The difference in peak weight loss rate between the calculated results and experimental data in nitrogen is within 10% for the four different heating rates. A small weight loss by char pyrolysis is noticeable above 400°C, but the difference is so small that char pyrolysis is not included for the overall gasification process in order to keep the degradation model as simple as possible. The calculated concentrations of CO, CO<sub>2</sub>, H<sub>2</sub>O, and HC (total hydrocarbons) in degradation products were compared with the experimental data; the results are shown in Figs. 10b, 10c, 10d, and 10e, respectively. These comparisons show reasonable agreement between model and experiment but with some discrepancies. Since the approximate approach of the constant yield for each degradation product during pyrolysis degradation was used in this study, temperature at peak values of these degradation generation is the same as the temperature at the peak weight loss rate. However, careful observation indicates that water tends to be generated at first followed by CO<sub>2</sub> and CO. This trend is consistent with previous more detailed studies [4, 8]. There is a significant difference in temperature at the CO peak between the calculated result and the experimental data. Although CO tends to

be generated later than water, this large shift could be caused by overlapping of CO generation from pyrolysis of char. During char pyrolysis roughly similar amounts of CO and CO<sub>2</sub> are generated. Since the amount of total hydrocarbons was derived from the difference between the sample weight loss and the summation of CO, CO<sub>2</sub>, and H<sub>2</sub>O in the experiment, its accuracy is not expected to be high. This is confirmed by the negative generation of HC after about 330°C shown in Fig. 10e. Therefore, unfortunately, the accuracy of the HC yield is the least certain in this study.

Calculated weight loss rates for oxidation degradation were compared with the experimental data and a typical comparison is shown in Fig. 11a. This condition was selected due to its mid range heating rate and oxygen concentration. The comparison for the all conditions of heating rates and oxygen concentrations used in the experiment indicate that calculated peak weight loss rates for the first peak in Fig. 11a are within 10% of the experimentally measured values and the calculated temperatures at the peak are within 4°C of the experimental values. However, calculated sample weight loss rates for char oxidation in 0.28% oxygen concentration tend to be slightly overestimated. Another difference between model and experiment is seen in the temperature range from 340° to 420°C. The experimental data show substantial weight loss rates but the calculated results are much less. This difference could be caused by broader char oxidation reaction than one-step global char oxidation kinetics used in the model and also pyrolysis of char, which is not included in the model. As shown later, this difference caused significant error in predicting CO and CO<sub>2</sub> generation in this temperature range. The difference was observed in all conditions measured in this study.

A comparison in evolved concentration of several degradation products between the experimental data and the calculated results is shown in Fig. 11b for CO, Fig. 11c for CO<sub>2</sub>, Fig. 11d for H<sub>2</sub>O, Fig. 11e for total hydrocarbons, and Fig. 11f for oxygen consumption. The calculated maximum CO concentrations for oxidative degradation and for char oxidation are close to those for the experimental data, but the gas is evolved at a lower temperature than in the experimental data for oxidative degradation reaction. Experimental

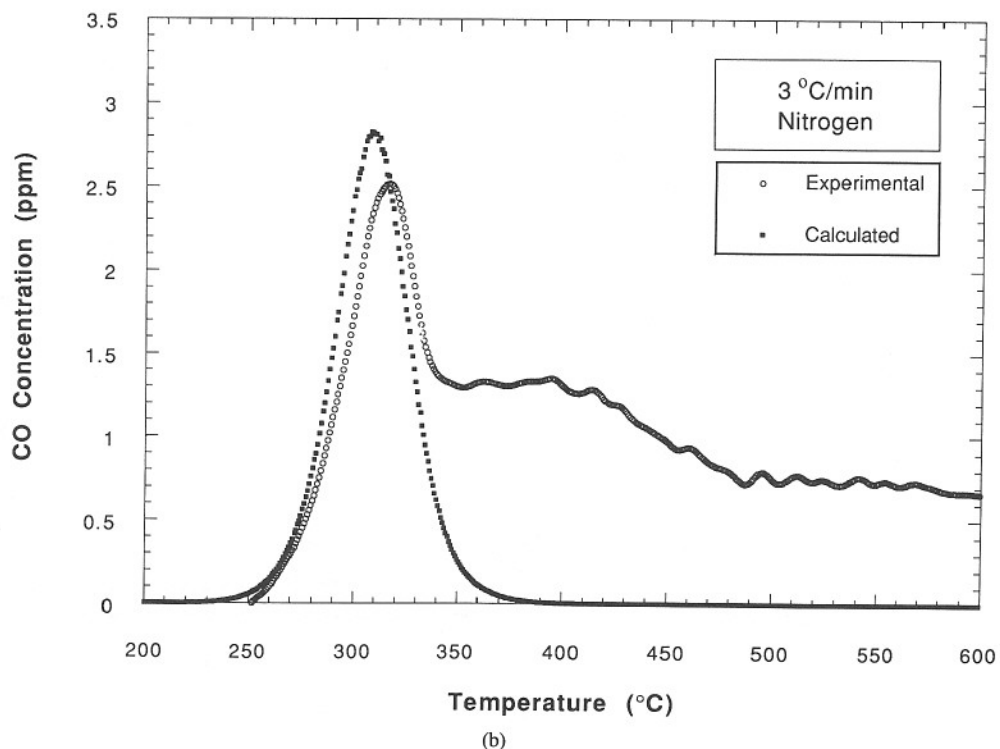
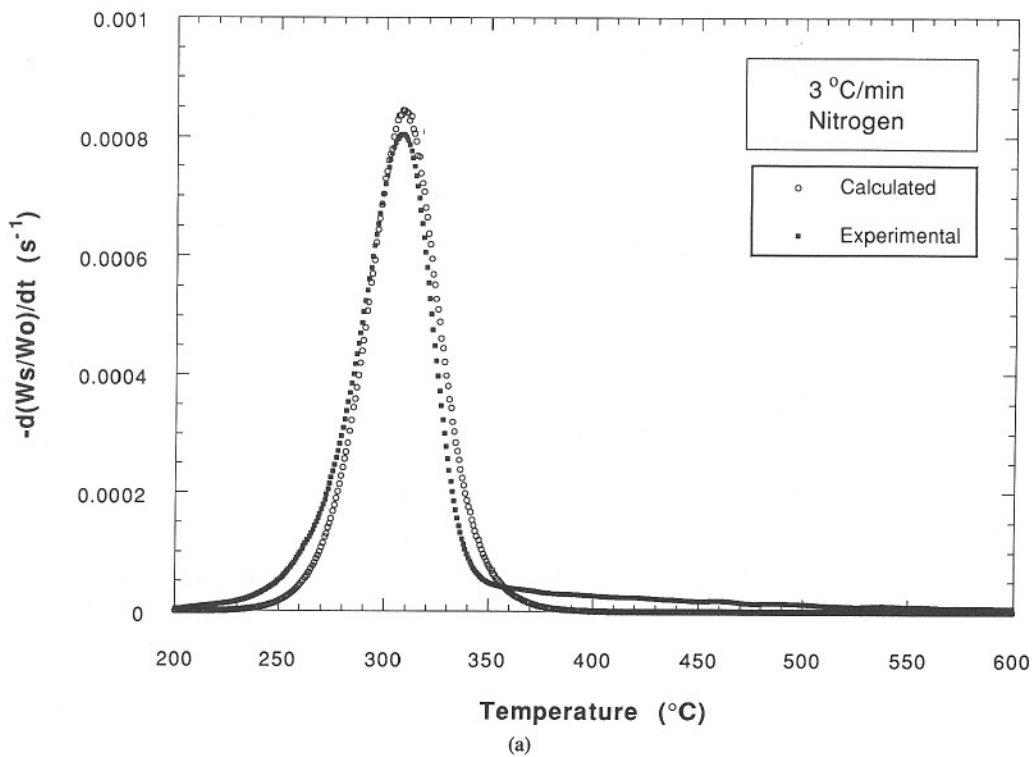


Fig. 10. Comparison of the calculated results with the experimental data at 3  $^{\circ}C/m$  heating rate in nitrogen, (a) sample weight loss rate, (b) CO, (c) CO<sub>2</sub>, (d) H<sub>2</sub>O, and (e) total hydrocarbons.

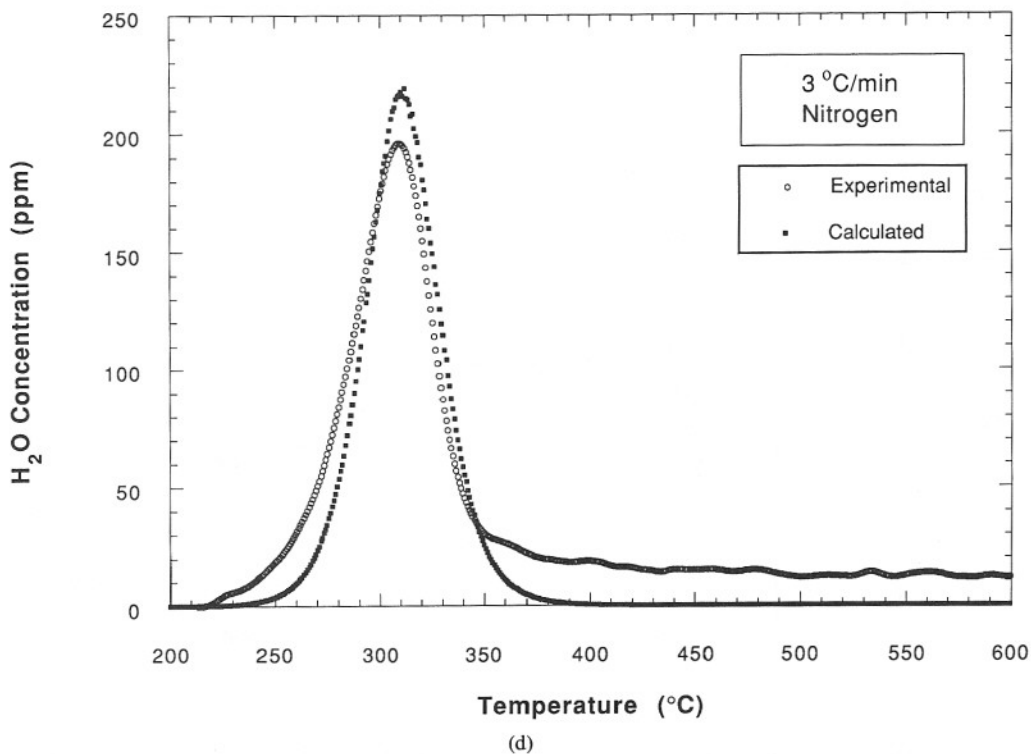
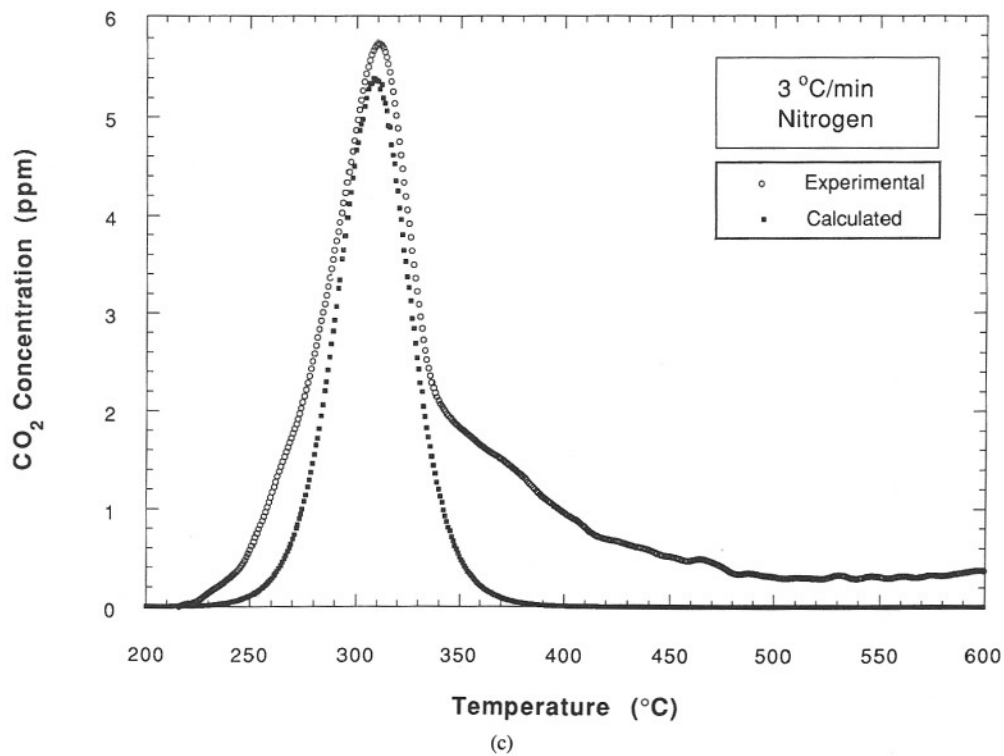
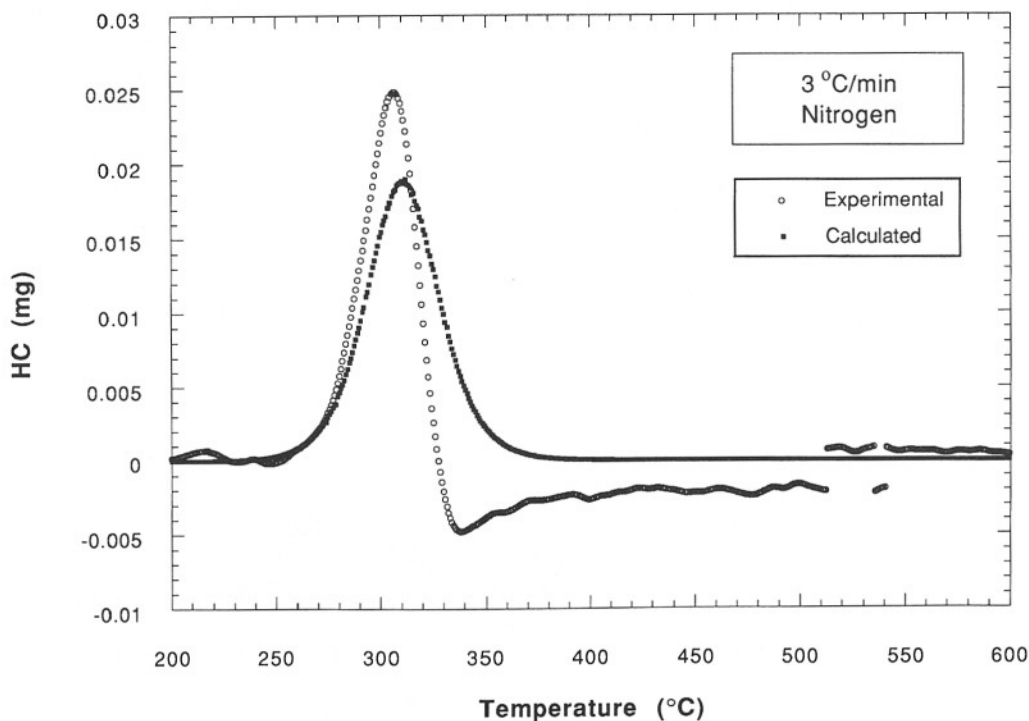


Fig. 10. (Continued).



(e)

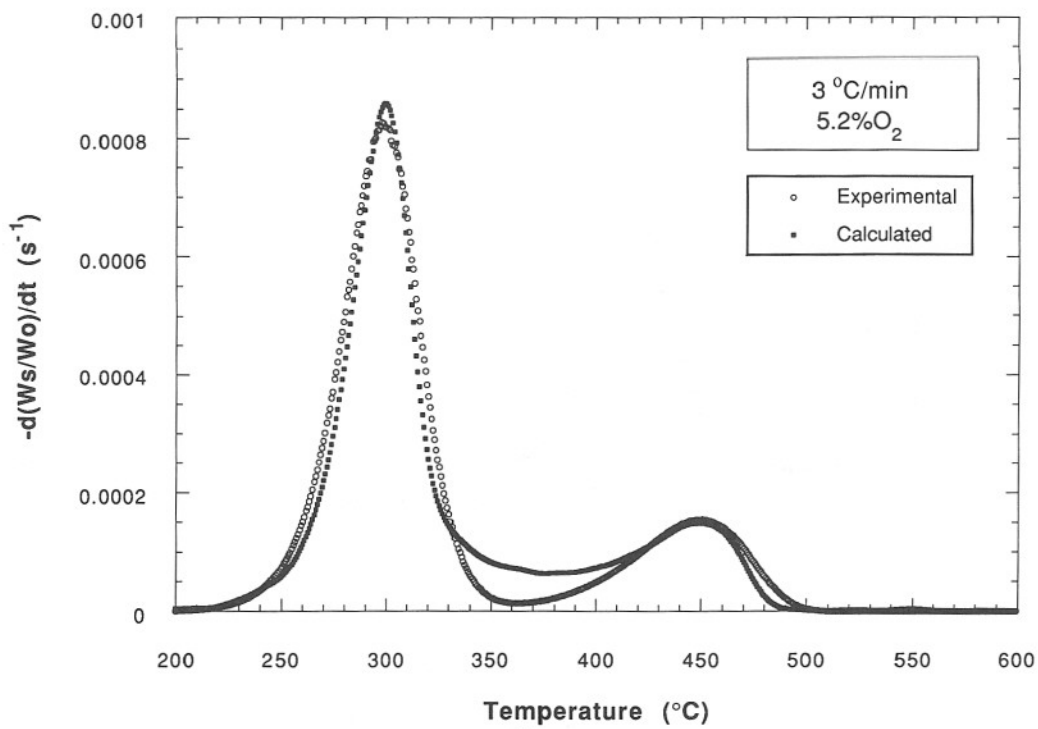
Fig. 10. (Continued).

CO concentrations in the temperature range from 340° to 420°C are much higher than the calculated results. This trend is also observed in all conditions studied in this study and furthermore the results for CO<sub>2</sub> show the same trend in Fig. 11c. This difference could be caused by the fact that the char oxidation used in this study is broader than one-step global char oxidation, as discussed above. [Since amounts of CO and CO<sub>2</sub> produced by pyrolysis of char are much smaller than those produced by char oxidation (Figs. 10b and 10c), pyrolysis of char can be neglected.] The calculated H<sub>2</sub>O concentrations are reasonably close to the experimental data with a slight shift to lower temperature at their maximum. However, the calculated results are much less than the experimental data in the temperature range from 340° to 420°C, similar to the CO and CO<sub>2</sub> case. Since the amount of H<sub>2</sub>O generated by pyrolysis of char is comparable to the results shown in Fig. 11d, in this case pyrolysis of char may be needed to predict H<sub>2</sub>O concentration. However, since water is only a diluent and its generation above 500°C is small, pyrolysis of char can be ne-

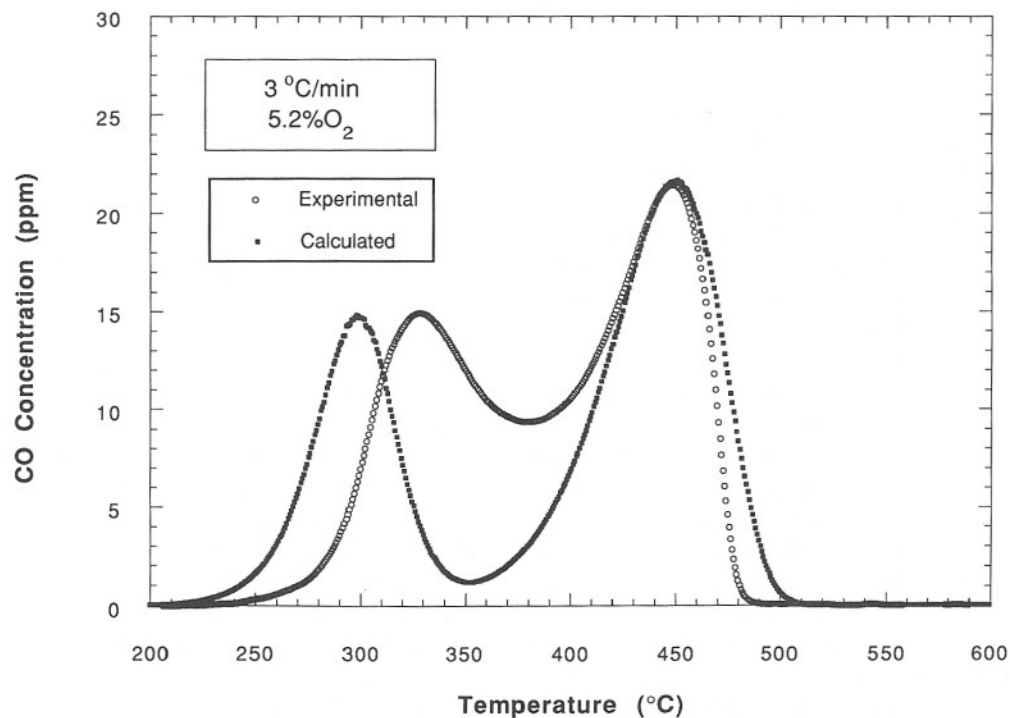
glected for a model to predict ignition and subsequent flame spread to keep the model tractable.

Since small amounts of oxygen consumption must be measured and counted for the mass balance to calculate total hydrocarbons, the experimental data for total hydrocarbons are not accurate enough to compare with the calculated results except near the oxidation/pyrolysis peak. The consumption of oxygen was measured by stretching the capability of the oxygen analyzer to its limit due to extremely small drop in oxygen concentration and its accuracy in the measured range is not expected to be high.

Nevertheless, the measured results show clear trend of oxygen consumption. Although calculated oxygen consumptions by char oxidation agree reasonably well with the measured results, the calculated oxygen consumptions by oxidative degradation occur at too low a temperature compared with the experimental data. This trend is consistent with the above-discussed trend for CO and CO<sub>2</sub> concentration. This indicates that the approach used in this study, in which all degradation products are generated proportional to the



(a)



(b)

Fig. 11. Comparison of the calculated results with the experimental data at 3 °C/m heating rate in 5.2% ambient oxygen concentration, (a) sample weight loss rate, (b) CO, (c) CO<sub>2</sub>, (d) H<sub>2</sub>O, (e) total hydrocarbons, and (f) oxygen consumption.

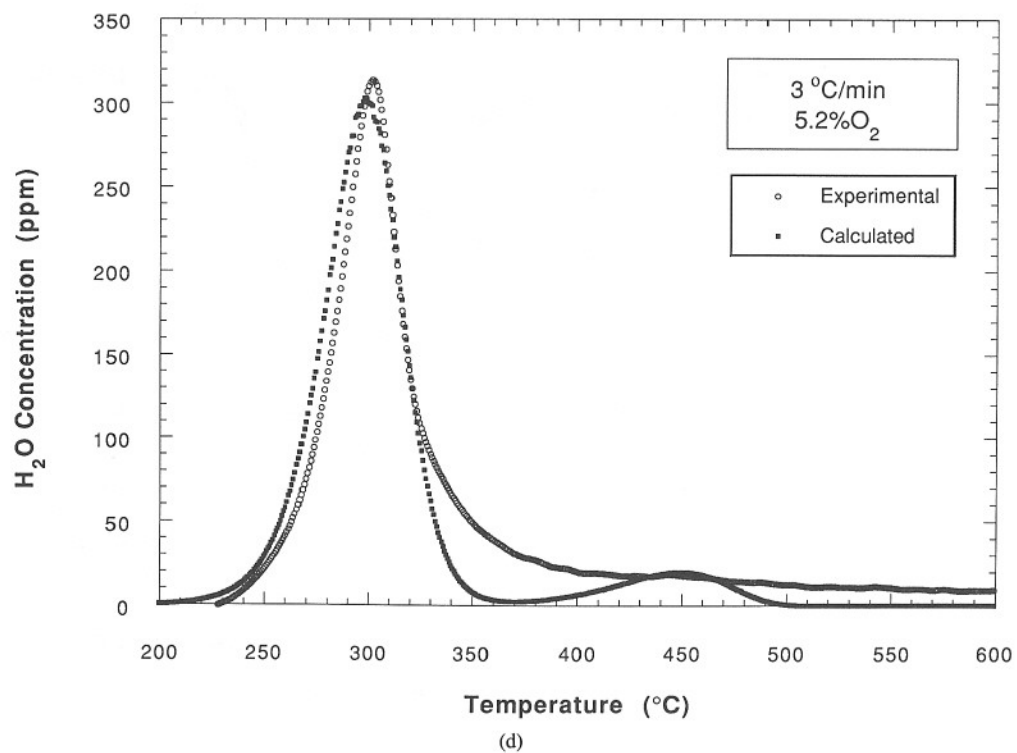
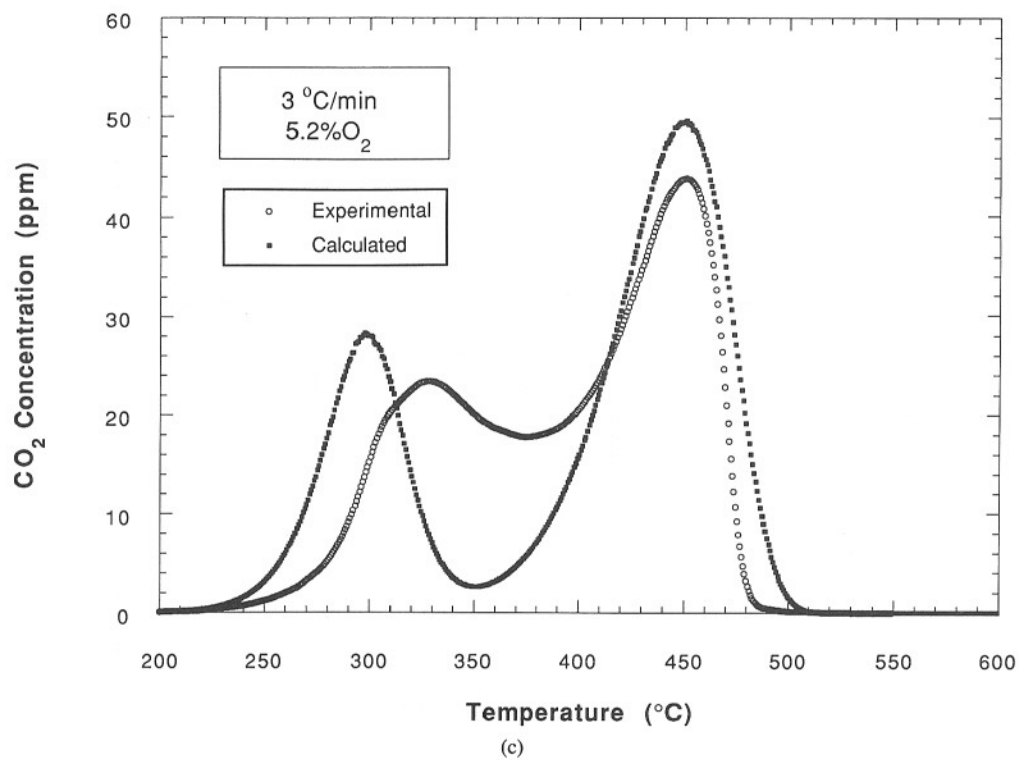


Fig. 11. (Continued).

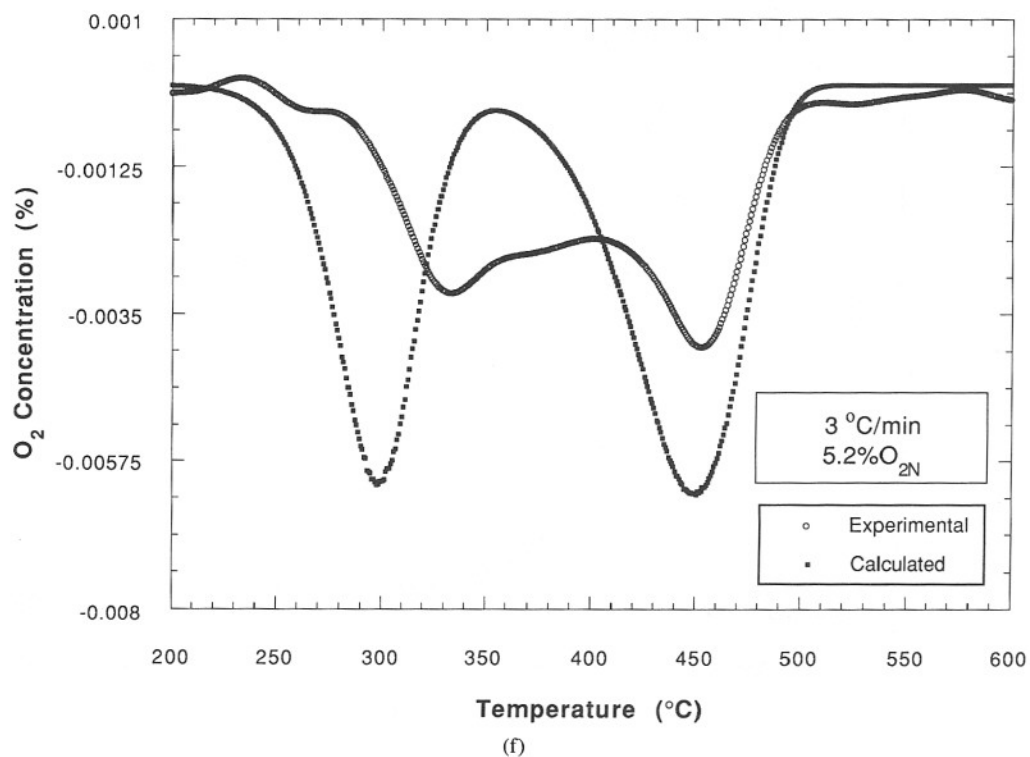
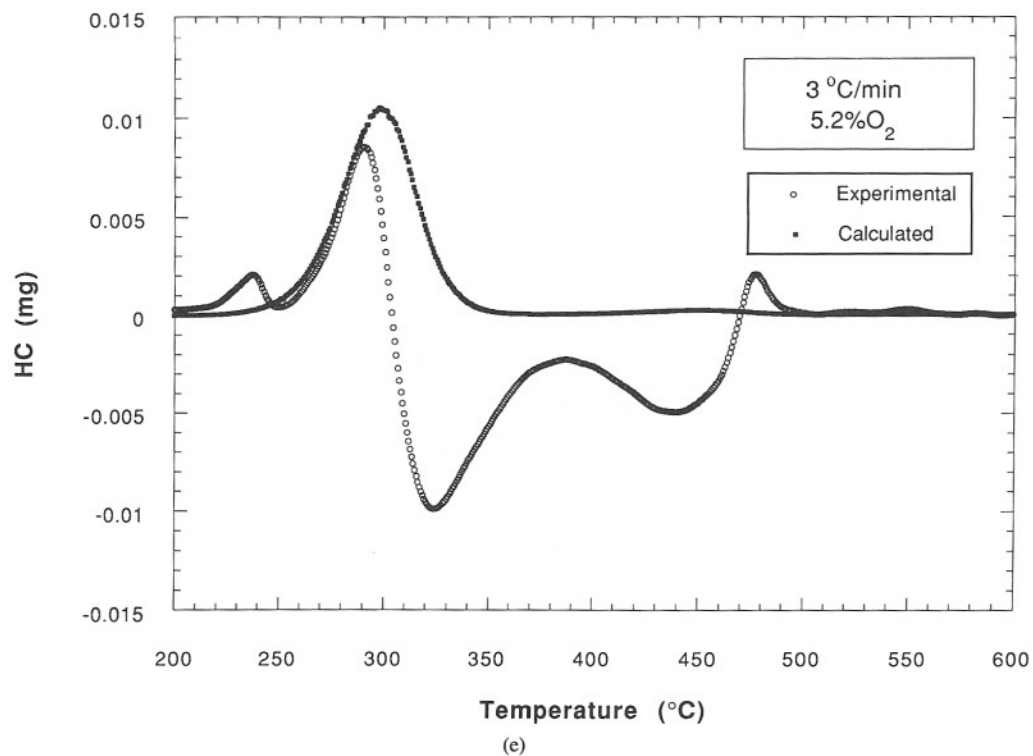


Fig. 11. (Continued).

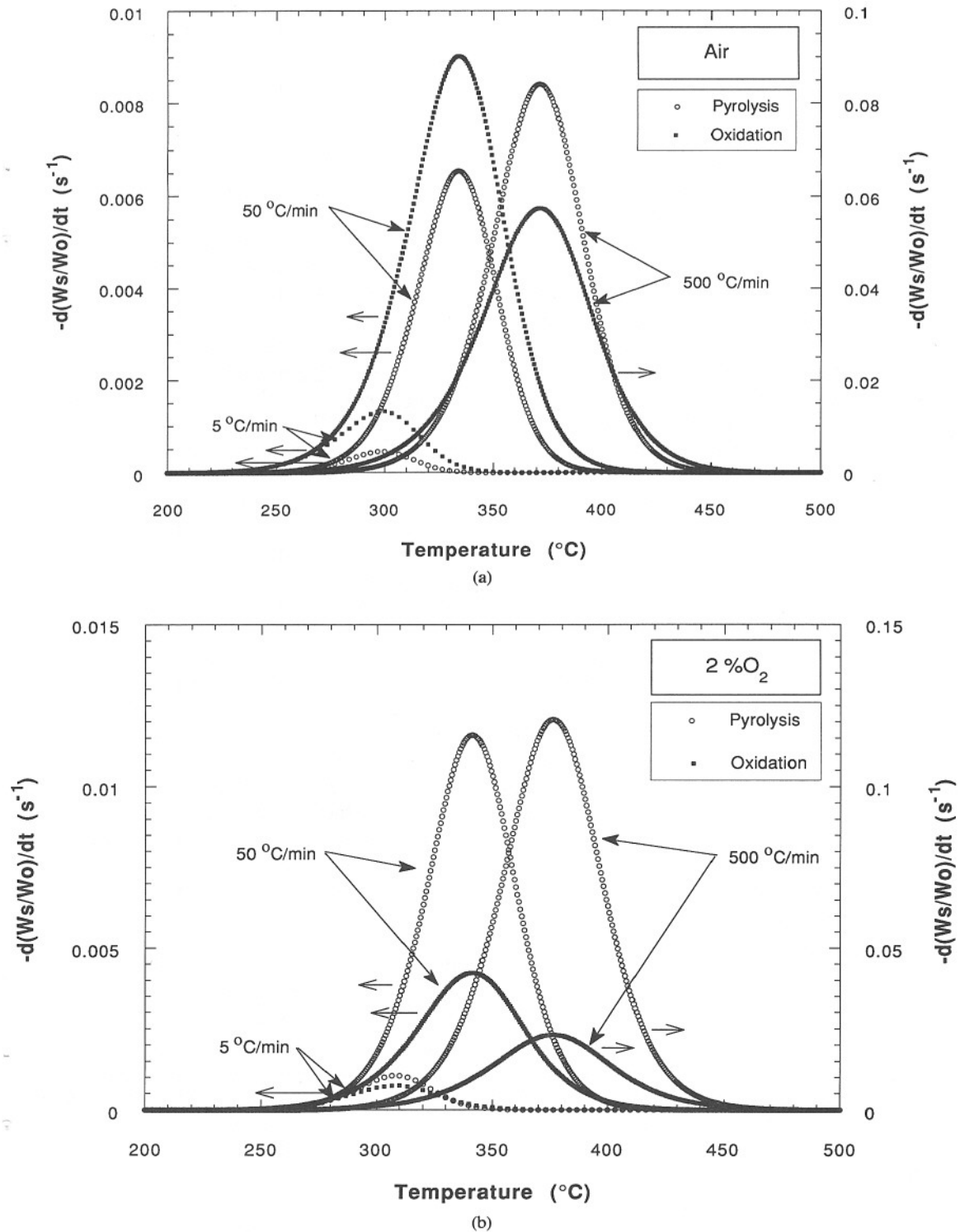


Fig. 12. Effects of heating rate on competition between pyrolysis rate and oxidative degradation rate, (a) in air and (b) 2% ambient oxygen concentration.

weight loss of the sample, is not accurate when applied to these two species. Although the approach is the simplest, the results show that CO and CO<sub>2</sub> are produced at the different stage of degradation for H<sub>2</sub>O. Another approach might be to use CO or CO<sub>2</sub> data to determine their oxidative kinetic constants, but this makes more complex expression and greatly increases numbers of constants. Another potential improvement to the approach used in this study is that mass addition to the sample by oxygen addition to the sample should be subtracted from sample weight for the determination of oxidative degradation kinetic constants. The estimated oxygen mass addition during oxidative degradation is up to about 10% of the sample weight (However, it is not clear what fraction of consumed oxygen actually contributes to the sample weight. This depends on the competition between rate of oxygen attack on the sample and rate of gasification of oxygen-attached degradation products.) Furthermore, in order to measure accurately the amounts of oxygen consumed by the oxidative degradation reaction requires a more sensitive oxygen analyzer than the one used in this study (maximum span of 0.5% oxygen concentration differential with reproducibility within 0.5% of the span).

This study was conducted using a conventional thermal gravimetric analyzer. Heating rates used in this study were quite low to assure that any transport effects on derived global kinetic constants were negligible. However, heating rates during the ignition period and subsequent flame spread in a microgravity environment will be two to three orders of magnitude higher than those used in this study. This raises a question as to the validity of application of the values of kinetic constants determined in this study to microgravity experiments. A recent experimental study [18] indicates that global kinetic constants for cellulose pyrolysis are the same for heating rates of 5°, 100°, and 1000°C/m and also agree with the data determined from experiments using heating rates up to 10,000°C/s [19]. However, the char yield determined from the extremely high heating rate experiments was zero [19], compared with values of 0.10–0.36 determined by low heating rate experiments [8, 9, 18]. This indicates that the composition of degradation products might be affected by heating rates, but global kinetic constants (weight loss rates) might not be affected by

heating rates. Further studies are needed to draw a firm conclusion on this matter.

In the previous study [18] it was observed that ambient oxygen effects on weight loss rate of cellulose diminished gradually with an increase in heating rate. Using the above derived kinetic constants for pyrolysis and oxidative degradation reactions (no char oxidation included), effects of heating rate on the competition between the two degradation reactions were studied by calculating weight loss rate for each degradation reaction using Eqs. 2 and 3. The assumption in this calculation was that oxygen supply was fast enough that ambient oxygen concentration did not change during degradation. The results for air (Fig. 12a) indicate that the oxidative degradation rate is roughly three times as large as the pyrolysis rate for 5°C/m. At 50°C/m the two rates are nearly equal and at 500°C/m the pyrolysis rate exceeds the oxidative degradation rate. This trend is mainly due to difference in activation energy between the two degradation reactions. Higher heating rate shifts the weight loss rate peak toward higher temperature, which enhances the pyrolysis rate more with its larger activation energy (220 kJ/mol) than that (160 kJ/mol) for the oxidative degradation reaction. Since the exothermicity of oxidative degradation is about ten times as large as endothermicity of the pyrolysis reaction, the overall degradation of the paper is slightly exothermic in air as long as the oxygen supply to the degrading paper is sufficient. If oxygen supply is not fast enough, the ambient oxygen concentration near the paper would be reduced. Such a case was considered and calculated in 2% ambient oxygen concentration, and the results are shown in Fig. 12b. The pyrolysis rate is higher than the oxidative degradation rate even at 5°C/m because the oxidative degradation rate becomes lower due to the low ambient oxygen concentration and the pyrolysis rate increases due to more available sample mass (less consumption by oxidative degradation reaction). This is the reason that the measured activation energies at 1.08 and 0.28% ambient oxygen concentrations were close to that for the pyrolysis reaction. It is interesting to note that higher ambient oxygen concentration does not significantly affect the peak total sample weight loss rate, but it shifts the peak toward lower temperature.

The consistency between the yields of the

degradation products and heat of reaction was examined by calculating each heat of reaction using heats of formation of the degradation products. The paper was assumed to consist of molecules of  $C_6H_{10}O_5$  and its heat of formation could be calculated using the measured heat of complete combustion, 4,165 J/g[21], and heats of formation of  $H_2O$  and  $CO_2$ . The derived heat of formation of the paper was  $-6000$  J/g. Although the heat of formation of the hydrocarbons could not be estimated without knowing their composition, their contribution to the energy balance for oxidative degradation (Eq. 3) and for char oxidative degradation (Eq. 5) was assumed to be small due to their small quantities in the degradation products. Using the above heat of formation for the paper and heat of formation of each reactant and products shown in Eq. 3, exothermic heats of 9200 J/g for oxidative degradation and of 22,500 J/g for char oxidation were obtained. The measured value for the oxidative reaction by DSC listed in Table 1 was exothermic 5700 J/g and it was exothermic 25,000 J/g for the char oxidation. The difference for oxidative degradation could be the neglected hydrocarbons in the calculation, and also water in products might be overestimated. The agreement for char oxidation is reasonable.

## CONCLUSION

Global kinetic constants for pyrolysis, oxidative degradation, and char oxidation reactions for paper were determined. The calculated peak sample weight loss rate for pyrolysis and oxidative degradation reactions using the kinetic constants are within 10% of the experimental data and the calculated temperature at the peak sample weight loss rate is within  $4^\circ C$  of the experimental data. However, the derived kinetic constants in the temperature range of  $340$ – $420^\circ C$  (at heating rates used in this study) underestimate weight loss rates.

Yields of  $H_2O$ ,  $CO$ ,  $CO_2$ , and total hydrocarbons in the degradation products were quantified by assuming that they do not vary during the degradation reactions. Although the calculated concentrations of these gases in the degradation products using these yields are close to experimental data for oxidative degradation, calculated  $CO$  and  $CO_2$  peaks are shifted toward lower temperature than experimental results. This is

probably due to formation of these gases at the later stage of degradation reactions than sample weight loss, which is initially dominated by loss of water.

The results indicate that combustible gases, total hydrocarbons and  $CO$ , in the degradation products are relatively small, about 23% for the pyrolysis reaction and 16% for the oxidative degradation (mass base). The rest of the degradation products are noncombustible.

*This study is supported by the NASA Microgravity Science Program under the Inter-Agency Agreement No. C-32000-K. The authors would like to thank for Mrs. Robin Breese and Mr. Chris Tate for their assistance in writing computer programs for taking data and making graphics.*

## REFERENCES

1. Kushida, G., Baum, H. R., and Kashiwagi, T., *J. Heat Transf.* (submitted).
2. Kushida, G., Baum, J. R., Yamashita, H., and Kashiwagi, T., (in preparation).
3. Friedman, R., and Sacksteder, K. K., NASA TM 88933 or AIAA-87-0467 (1987).
4. Shafizadeh, F., *J. Anal. Appl. Phys.* 3:283–305 (1982).
5. Nakagawa, S., and Shafizadeh, F., in *Hand Book of Physical and Mechanical Testing of Paper and Paperboard* (R. E. Marks, Ed.), Marcel Dekker, New York, 1984, Vol. 2, chap. 23.
6. Martin, S., *Tenth Symposium (International) on Combustion*, The Combustion Institute, Pittsburgh, 1965, 877–896.
7. Lipska, A. E., and Parker, W. J., *J. Appl. Polym. Sci.* 10:1439–1453 (1966).
8. Broido, A., and Nelson, M. A., *Combust. Flame* 24:263–268 (1975).
9. Shafizadeh, F., and Bradbury, A. G. W., *J. Appl. Polym. Sci.* 23:1431–1442 (1979).
10. Jain, R. K., Lal, K., and Bhatnager, H. L., *J. Appl. Polym. Sci.* 30:897–914 (1985).
11. Dollimore, D., and Hoath, M. J., *Thermochim. Acta* 121:273–282 (1987).
12. Rogers, F. E., and Ohlemiller, T. J., *Combust. Sci. Technol.* 24:129–137 (1980).
13. Kashiwagi, T., Hirata, T., and Brown, J. E., *Macromolecules* 18:131–138 (1985).
14. Flynn, J. H., and Wall, L. A., *J. Res. Nat. Bur. of Stand.* 70A:487–523 (1966).

15. Bradbury, A. W., Sakai, Y., and Shafizadeh, F., *J. Apply. Polym. Sci.* 23:3271-3280 (1979).
16. Kissinger, H. E., *Anal. Chem.* 29:1702-1706 (1957).
17. Lewellen, P. C., Peters, W. A., and Howard, J. B., *Sixteenth Symposium (International) on Combustion*, The Combustion Institute, Pittsburgh, 1976, pp. 1471-1480.
18. Suuberg, E. M., and Dalal, V. F., 1987 Eastern States Combustion Institute Meeting, November 1987.
19. Shivadev, U. K., and Emmons, H. W., *Combust. Flame* 22:223-236 (1974).
20. Tang, W. K., and Neil, W. K., *J. Polymer. Sci.* 6C:65-81 (1964).
21. Domalski, E. S., Evans, W. H., and Jobe, T. L., NBSIR 78-1479, August 1978.

*Received 10 June 1991; revised 16 September 1991*